PHYSICAL REVIEW LETTERS

Spontaneous Quantum Hall States in Chirally Stacked Few-Layer Graphene Systems

Fan Zhang,[1,*] Jeil Jung,[1] Gregory A. Fiete,[1] Qian Niu,[1,2] and Allan H. MacDonald[1]

[1]*Department of Physics, University of Texas at Austin, Austin, Texas 78712, USA*
[2]*International Center for Quantum Materials, Peking University, Beijing 100871, China*
(Received 19 October 2010; published 11 April 2011)

Chirally stacked N-layer graphene systems with $N \geq 2$ exhibit a variety of distinct broken symmetry states in which charge density contributions from different spins and valleys are spontaneously transferred between layers. We explain how these states are distinguished by their charge, spin, and valley Hall conductivities, by their orbital magnetizations, and by their edge state properties. We argue that valley Hall states have $[N/2]$ edge channels per spin valley.

PACS numbers: 73.43.−f, 71.10.−w, 73.21.−b, 75.76.+j

Introduction.—In the early 1980s, following the discovery of the quantum Hall effect [1], it was recognized [2] that electronic states can be characterized by topological indices, in particular, by the integer-valued Chern number indices that distinguish quantum Hall states. Quantum Hall states have nonzero Chern numbers and can occur only if time-reversal symmetry is broken; until recently, they have been observed only when time-reversal symmetry is explicitly broken by an external magnetic field. In this Letter, we discuss a class of broken symmetry states, first proposed theoretically [3–5] and recently discovered experimentally [6,7], which appear in chirally stacked graphene systems and are characterized by spin- and valley-dependent spontaneous layer polarization. The aim of the present Letter is to explain how these states are distinguished by their charge [8–10], spin [11], and valley [12] quantized Hall conductances, by their orbital magnetizations, and by their edge state properties.

Success in isolating monolayer and few-layer sheets from bulk graphite, combined with progress in the epitaxial growth of few-layer samples, has opened up a rich new topic [13] in two-dimensional electron physics. Electron-electron interaction effects are most interesting in *ABC*-stacked $N \geq 2$ layer systems [14–16], partly because [3,4,17–20] their conduction and valence bands are very flat near the neutral system Fermi level. For this special stacking order, low-energy electrons are concentrated on the top and bottom layers, and the low-energy physics of a N-layer system is described approximately by a two-band model with $\pm p^N$ dispersion and large associated momentum-space Berry curvatures [21]. When these band states are described in a pseudospin language, the broken symmetry state is characterized [3] by a momentum-space vortex with vorticity N and a vortex core which is polarized in the top or bottom layers. For *AB*-stacked bilayers, for example, interactions lead to a broken symmetry ground state [3,4,19] with a spontaneous gap in which charge is transferred between the top and bottom layers. *ABC*-stacked trilayer graphene has even flatter bands and is expected to be even more unstable to

interaction-driven broken symmetries [16], but samples that are clean enough to reveal its interaction physics have not yet been studied.

Hall conductivities and magnetizations.—We discuss the electronic properties of N-layer *ABC*-stacked systems by using the ordered state quasiparticle Hamiltonians suggested by mean-field calculations [3,19] and renormalization group analysis [4]:

$$\mathcal{H}_N = \frac{(v_0 p)^N}{(-\gamma_1)^{N-1}} [\cos(N\phi_{\boldsymbol{p}})\sigma_x + \sin(N\phi_{\boldsymbol{p}})\sigma_y] + \lambda\sigma_z.$$

(1)

We have used the notation $\cos\phi_{\boldsymbol{p}} = \tau_z p_x/p$ and $\sin\phi_{\boldsymbol{p}} = p_y/p$, where $\tau_z = \pm 1$ labels valleys K and K', the two inequivalent Brillouin zone corners. The Pauli matrices $\boldsymbol{\sigma}$ act on a *which-layer* pseudospin degree of freedom, and $s_z = \pm 1$ denotes the two spin flavors. In Eq. (1) the first term [14,16] is the low-energy $\mathbf{k} \cdot \mathbf{p}$ band Hamiltonian for a single valley. Weak remote hopping processes have been dropped with the view that they do not play an essential role in the broken symmetry states [4]. The second term is an interaction-induced gap [3,4,19,20] term which defines the direction of layer polarization in the momentum-space vortex core. Since the pseudospin chirality frustrates off-diagonal symmetry breaking [3], we consider only the pertinent types of diagonal symmetry breaking. For each spin and valley, symmetry is broken by choosing a sign for λ. We have dropped the momentum dependence of λ because, as we will see, it does not play an essential role below. $2|\lambda|$ is the size of the spontaneous gap, v_0 is the Fermi velocity in graphene, and $\gamma_1 \sim 0.4$ eV is the interlayer hopping energy. The p^N dispersion is a consequence of the N-step process in which electrons hop between low-energy sites in top and bottom layers via high-energy states.

When spin and valley degrees of freedom are taken into account, the system has 16 distinct broken symmetry states in which the sign of λ is chosen separately for $(K\uparrow)$, $(K\downarrow)$, $(K'\uparrow)$, and $(K'\downarrow)$ flavors. We take the view that any of these states could be stable, depending on details

that are beyond current knowledge and might be tunable experimentally. The 16 states can be classified according to their total layer polarization, which is proportional to the sum over the spin valley of the sign of λ. Six of the 16 states have no net layer charge transfer between the top and bottom layers and are likely to be lowest in energy in the absence of an external electric field. These six states can be separated into three doublets which differ only by layer inversion in every spin valley. Thus three essentially distinct states compete for the broken symmetry ground state: the anomalous Hall state in which the sign of λ is valley-dependent but not spin-dependent ($\lambda\sigma_z \to \lambda\tau_z\sigma_z$), the layer-antiferromagnetic state in which λ is only spin-dependent ($\lambda\sigma_z \to \lambda s_z\sigma_z$), and the topological insulator (TI) state in which λ is both spin- and valley-dependent ($\lambda\sigma_z \to \lambda\tau_z s_z\sigma_z$). These states are distinguished by their spin- and valley-dependent Hall conductivities and orbital magnetizations indicated schematically in Fig. 1 and summarized in Table I.

Berry curvatures.—The three broken symmetry states on which we focus are distinguished by the signs of the Berry curvatures [21] contributions from near the K and K' valleys of ↑ and ↓ spin bands; we note that the Berry curvatures are nonzero only when inversion symmetry is
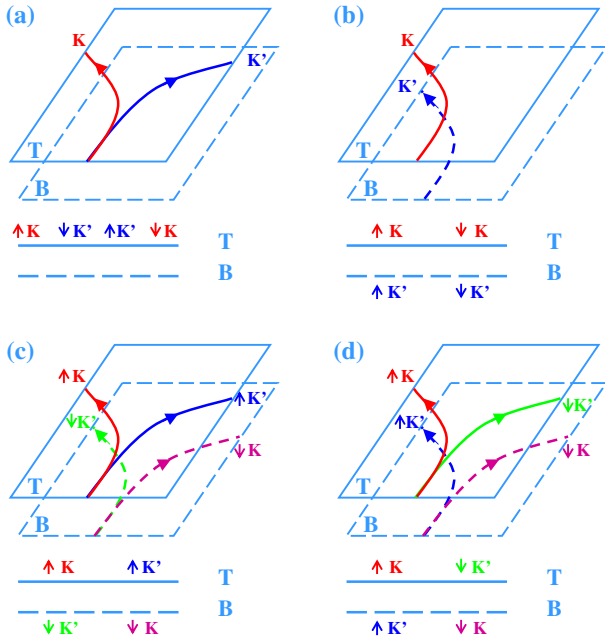
FIG. 1 (color online). For cases (a)–(d) the lower panel describes the sense of layer polarization for each spin-valley combination, while the upper panel schematically indicates the corresponding Hall conductivity contributions. (a) A valley Hall (QVH) insulator with a net layer polarization and a charge-density wave mass $\lambda\sigma_z$; (b) an anomalous Hall (QAH) insulator with a valley-dependent mass $\lambda\tau_z\sigma_z$; (c) a layer-antiferromagnetic (LAF) insulator with a spin-dependent mass $\lambda s_z\sigma_z$; (d) a quantum spin Hall (QSH) insulator (or a 2D TI) with a valley- and spin-dependent mass term $\lambda\tau_z s_z\sigma_z$.

spontaneously broken. Using the Berry curvatures, we evaluate the orbital magnetizations and Hall conductivities of all three states. For momentum-independent mass λ, the Berry curvature of the N-layer chiral model is

$$\Omega_{\hat{z}}^{(\alpha)}(\boldsymbol{p}, \tau_z, s_z) = -\alpha \frac{\tau_z}{2} \frac{\lambda}{h_t^3}\left(\frac{\partial h_\|}{\partial p}\right)^2, \qquad (2)$$

where the symbol $\alpha = +(-)$ denotes the conduction (valence) band and the transverse and total pseudospin fields are $h_\| = (v_0 p)^N / \gamma_1^{N-1}$ and $h_t = \sqrt{\lambda^2 + h_\|^2}$. The orbital magnetic moment carried by a Bloch electron [21] is $m_{\hat{z}}^{(\alpha)} = e\hbar\varepsilon^{(\alpha)}\Omega_{\hat{z}}^{(\alpha)}$ for a two-band model with particle-hole symmetry. For the chiral band model

$$m_{\hat{z}}^{(\alpha)}(\boldsymbol{p}, \tau_z, s_z) = \left[-\tau_z \frac{\lambda}{h_t^2}\left(\frac{\partial h_\|}{\partial p}\right)^2 m_e\right]\mu_B, \qquad (3)$$

where m_e is the electron mass and μ_B is the Bohr magneton $e\hbar/2m_e$. Like the Berry curvature, the orbital magnetization changes sign when the valley label changes *and* when the sign of the mass term (the sense of layer polarization) changes; i.e., both are proportional to $\tau_z\mathrm{sgn}(\lambda)$. The orbital magnetization is, however, independent of the band index α. As illustrated in Fig. 2, in the case of $|\lambda| = 10$ meV, the orbital magnetic moment close to each Dirac point has a symmetric sharp peak at which individual states carry moments 20 times larger than μ_B. The state in which $\lambda \to \lambda\tau_z$ therefore has overall orbital magnetization and broken time-reversal symmetry, even though it does not have a finite spin polarization. Integrating over the valence band, we obtain a total orbital magnetization per area $\sim(N\lambda m_e/2\pi\hbar^2)\ln(\gamma_1/|\lambda|)\mu_B$, that is, $\sim 0.002\mu_B$ per carbon atom for $|\lambda| = 10$ meV.

In the presence of an in-plane electric field, an electron acquires an anomalous transverse velocity proportional to the Berry curvature, giving rise to an intrinsic Hall conductivity [9,21]. Using Eq. (3), we find that the intrinsic Hall conductivity contribution from a given valley and spin is

$$\sigma_H^{(\alpha)}(\tau_z, s_z) = \frac{\tau_z}{2}\frac{Ne^2}{h}\left(\frac{\lambda}{h_t(p_F)} - \frac{\lambda}{|\lambda|}\delta_{\alpha,+}\right), \qquad (4)$$

TABLE I. Summary of spin-valley layer polarizations (T or B) and corresponding charge, spin, and valley Hall conductivities (e^2/h units) and insulator types for the three distinct states (b)–(d) with no overall layer polarization on which we focus, for a state in which every spin valley is polarized toward the top layer (a) and for a state with partial layer polarization.

Fig.	$K\uparrow$	$K\downarrow$	$K'\uparrow$	$K'\downarrow$	$\sigma^{(\mathrm{SH})}$	$\sigma^{(\mathrm{VH})}$	$\sigma^{(\mathrm{CH})}$	$\sigma^{(\mathrm{SVH})}$	Insulator
1(b)	T	T	B	B	0	0	$2N$	0	QAH
1(c)	T	B	T	B	0	0	0	$2N$	LAF
1(d)	T	B	B	T	$2N$	0	0	0	QSH
1(a)	T	T	T	T	0	$2N$	0	0	QVH
	T	T	T	B	N	N	N	N	All
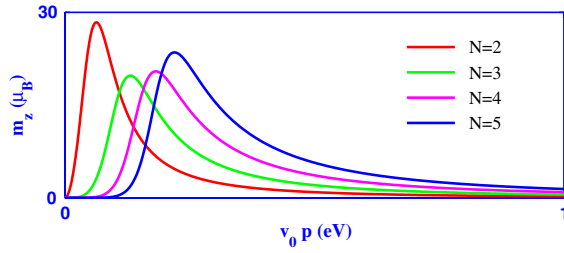
FIG. 2 (color online).   The magnitude of orbital magnetic moments carried by individual states versus in-plane momentum, for each spin and valley flavor in *ABC* graphene *N* layers. Here the moments are in units of μ_B and $|\lambda| = 10$ meV.

where $h_t(p_F)$ is the total pseudospin field at the Fermi wave vector. Provided that the Fermi level lies in the mass gap, each spin and valley contributes $Ne^2/2h$ to the Hall conductivity, with the sign given by $\tau_z \mathrm{sgn}(\lambda)$.

In Fig. 1(a), we consider the case in which each spin valley is polarized in the same sense. The total Hall conductivity is then zero for both spins, with the *K* and *K'* valleys making Hall conductivity and magnetization contributions of opposite sign, preserving time-reversal symmetry. This phase can be viewed as having a valley Hall effect [12], and, even though it does not break time-reversal symmetry, we argue later that this designation has physical significance.

As shown in Fig. 1(b), the case $\lambda\sigma_z \rightarrow \lambda\tau_z\sigma_z$ implies Hall conductivity and orbital magnetization contributions of the same sign for each spin and valley. This state breaks time-reversal symmetry, but its spin density is surprisingly everywhere zero. The total Hall conductivity has the quantized value $2Ne^2/h$. Similarly, the orbital magnetic moment has the same sign for all flavors. We refer to this state as the quantized anomalous Hall state. In addition to its anomalous Hall effect, this state has a substantial orbital magnetization. The anomalous Hall states is probably most simply identified experimentally by observing a $\nu = 2N$ quantum Hall effect which persists to zero magnetic field.

For $\lambda\sigma_z \rightarrow \lambda s_z\sigma_z$, depicted in Fig. 1(c), the two spins have valley Hall effects of opposite sign, and the two layers have spin polarizations of opposite sign. This layer-antiferromagnetic state has broken time-reversal symmetry and opposite spin polarizations on the top and bottom layers.

Figure 1(d) describes the third type of state with effective interaction $\lambda\sigma_z \rightarrow \lambda\tau_z s_z\sigma_z$. This state does not break time-reversal invariance and instead has anomalous Hall effects of opposite signs in the two spin subspaces, i.e., a spin Hall effect. Neither the top nor the bottom layer has spin or valley polarization. Quite interestingly, if we consider only one layer, there are both spin Hall and valley Hall effects; however, the orientations of the Hall currents in the top and the bottom layers are the same for the spin Hall effects but opposite for the valley Hall effects.

Table I includes as well the case in which one flavor polarizes in the opposite sense of the other three; charge, valley, and spin Hall effects coexist in this state, which can be favored by a small potential difference between the layers [20].

Edge states.—The physical significance of spontaneous charge, valley, and spin anomalous Hall effects is illustrated in Fig. 3. Graphene has very weak spin-orbit interactions, which in our case we ignore altogether. Figure 3 compares the edge electronic structure of $N = 1, 2, 3$ spinless models with a quantized anomalous Hall effect (i.e., with opposite layer polarizations at two valleys) and with a quantized valley Hall effect. The states with anomalous Hall effects have N topologically protected robust chiral edge states associated with the quantum Hall effect, as shown in Figs. 3(d)–3(f). The edge state structure associated with the valley Hall states is more interesting. In the $N = 1$ valley Hall state, the Hall conductivity contribution associated with each valley is $1/2$ in e^2/h units; the full unit of Hall conductance requires the two valleys to act in concert. Because they act in opposition in the valley Hall state, there is no edge state, as shown in Fig. 3(a). For $N = 2$, on the other hand, each valley contributes a full quantum Hall effect, and as we see in Fig. 3(b), we find two chiral edge states with opposite chirality, one associated with each valley. For $N = 3$, depicted in Fig. 3(c), the additional half quantum Hall effect from each valley is insufficient to produce a new chiral edge state branch. In general, we expect $[N/2]$ chiral edge state branches at each valley in an *N*-layer stack. Of course, valley Hall edge states are topologically protected only when the edge-direction projections of *K* and *K'* valleys are not coincident
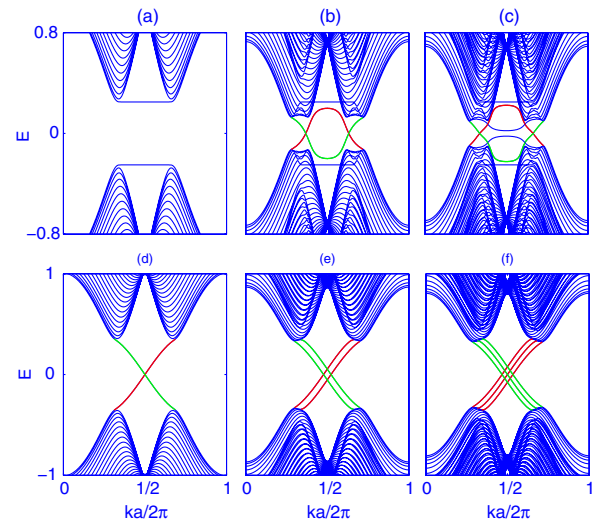
FIG. 3 (color online).   Intravalley and intervalley edge states in chirally stacked graphene systems. (a),(d) For a single layer, (b), (e) for a bilayer, and (c),(f) for a trilayer. To visualize the edge states, the intralayer and interlayer nearest neighbor hoppings are chosen as $\gamma_0 = 1$ and $\gamma_1 = 0.3$, respectively; $\lambda = 0.25$ for (a)–(c) and $\lambda = 0.3\sqrt{3}\tau_z$ for (d)–(f).

and intervalley scattering due to disorder is absent. Nevertheless, we expect robust edge states to be present in valley Hall states, as found [22] in numerical studies of valley Hall states induced by an external electric field without interactions.

Discussion.—At the level of the continuum-model mean-field theory [3], the three charge balanced states we have discussed are degenerate. In addition to breaking inversion symmetry, each breaks two of three additional symmetries: time reversal ($\mathcal{T}$), spin-rotational invariance [$SU(2)$], and the valley Ising symmetry ($\mathcal{Z}_2$). The TI state preserves only $\mathcal{T}$, the anomalous Hall phase preserves only spin-rotational invariance, and the antiferromagnetic state has $\mathcal{Z}_2$ symmetry. Both TI and antiferromagnetic phases break the continuous $SU(2)$ symmetry, and therefore Goldstone modes emerge [10]. The actual ground state is dependent on subtle correlation and microscopic physics issues that are beyond the scope of this paper. We note, however, that it might be possible to induce transitions between different possible states by using external fields. For example, the energy of the quantized anomalous Hall state will be lowered by a perpendicular external magnetic field because it has a large orbital magnetization. The fully layer polarized state will be favored by an external electric field which produces a potential difference between the layers. Increasing the magnetic field further results in quantum Hall ferromagnetism [23–25]. Recent experiments [6,7] in bilayers appear to provide definitive proof that the ground state at very weak external magnetic fields is the quantized anomalous Hall state.

The quantum spin Hall effect we discuss in this Letter is in several respects different from that discussed in the well known papers [5,11] which foreshadowed the identification of topological insulators. (i) The quantum spin Hall effect is driven by broken symmetries produced by electron-electron interactions, rather than by spin-orbit interactions [11], which we neglect. The effective spin-orbit coupling $\lambda\tau_z s_z \sigma_z$ due to electron-electron interactions can be 10^4 times larger than the intrinsic one [26]. (ii) Unlike the previous interaction-induced TI phase [5], which appears only at finite interaction strengths, here the instability to the TI phase is present even for weak interactions. (iii) The broken symmetry occurs only for $N \geq 2$ rather than in the single-layer systems [5,11]. (iv) Our states are also distinguished topologically, since they are characterized by Chern numbers which can have any integer value, rather than by a Z_2 label. Of course, only N-odd layers are topologically nontrivial TIs, because the helical edge modes are likely to localize in an N-even system due to the backscattering process allowed by $\mathcal{T}$ [27]. When Rashba spin-orbital interactions are strong, the spin Hall state is likely to be selected as the ground state and the Hall conductance will no longer be precisely quantized.

The estimated strength of Rashba spin-orbital interactions [26,28] in most experimental systems studied to date is much smaller than the estimated spontaneous gap [20], so its influence will normally be marginal.

*zhangfan@physics.utexas.edu

[1] K. Von Klitzing, G. Dorda, and M. Pepper, Phys. Rev. Lett. **45**, 494 (1980).
[2] D. J. Thouless *et al.*, Phys. Rev. Lett. **49**, 405 (1982).
[3] H. Min *et al.*, Phys. Rev. B **77**, 041407(R) (2008).
[4] F. Zhang *et al.*, Phys. Rev. B **81**, 041402(R) (2010).
[5] S. Raghu *et al.*, Phys. Rev. Lett. **100**, 156401 (2008); J. Wen *et al.*, Phys. Rev. B **82**, 075125 (2010).
[6] J. Martin *et al.*, Phys. Rev. Lett. **105**, 256806 (2010).
[7] R. T. Weitz *et al.*, Science **330**, 812 (2010).
[8] F. D. M. Haldane, Phys. Rev. Lett. **61**, 2015 (1988).
[9] N. Nagaosa *et al.*, Rev. Mod. Phys. **82**, 1539 (2010).
[10] R. Nandkishore and L. Levitov, Phys. Rev. B **82**, 115124 (2010).
[11] C. L. Kane and E. J. Mele, Phys. Rev. Lett. **95**, 226801 (2005); M. Konig *et al.*, Science **318**, 766 (2007).
[12] D. Xiao, W. Yao, and Q. Niu, Phys. Rev. Lett. **99**, 236809 (2007).
[13] A. H. Castro Neto *et al.*, Rev. Mod. Phys. **81**, 109 (2009).
[14] E. McCann and V. I. Fal'ko, Phys. Rev. Lett. **96**, 086805 (2006).
[15] Hongki Min and A. H. MacDonald, Phys. Rev. B **77**, 155416 (2008).
[16] F. Zhang *et al.*, Phys. Rev. B **82**, 035409 (2010).
[17] F. Guinea, Physics **3**, 1 (2010).
[18] O. Vafek and K. Yang, Phys. Rev. B **81**, 041401(R) (2010).
[19] R. Nandkishore and L. Levitov, Phys. Rev. Lett. **104**, 156803 (2010).
[20] J. Jung, F. Zhang, A. H. MacDonald, Phys. Rev. B, **83**, 115408 (2011).
[21] D. Xiao, M. Chang, and Q. Niu, Rev. Mod. Phys. **82**, 1959 (2010).
[22] J. Li *et al.*, Nature Phys. **7**, 38 (2011).
[23] Y. Barlas *et al.*, Phys. Rev. Lett. **101**, 097601 (2008).
[24] B. Feldman, J. Martin, and A. Yacoby, Nature Phys. **5**, 889 (2009).
[25] Y. Zhao *et al.*, Phys. Rev. Lett. **104**, 066801 (2010).
[26] H. Min *et al.*, Phys. Rev. B **74**, 165310 (2006).
[27] C. Xu and J. E. Moore, Phys. Rev. B **73**, 045322 (2006); E. Prada, P. San-Jose, and L. Brey, arXiv:1007.4910.
[28] W. Norimatsu and M. Kusunoki, Phys. Rev. B **81**, 161410 (R) (2010).